Neurobiology of Learning and Memory 135 (2016) 73–82

Contents lists available at ScienceDirect

Neurobiology of Learning and Memory

journal homepage: www.elsevier.com/locate/ynlme

Cognitive deficits in single *App* knock-in mouse models

Akira Masuda [a], Yuki Kobayashi [a], Naomi Kogo [a], Takashi Saito [b], Takaomi C. Saido [b], Shigeyoshi Itohara [a,*]

[a] Laboratory for Behavioral Genetics, Brain Science Institute, RIKEN, 2-1 Hirosawa, Wako, Saitama 351-0198, Japan
[b] Laboratory for Proteolytic Neuroscience, Brain Science Institute, RIKEN, 2-1 Hirosawa, Wako, Saitama 351-0198, Japan

ARTICLE INFO

Article history:
Received 13 April 2016
Revised 14 June 2016
Accepted 1 July 2016
Available online 1 July 2016

Keywords:
Alzheimer's disease
Model mouse
Cognition
IntelliCage
Sex
Amyloid precursor protein

ABSTRACT

Transgenic mouse models of Alzheimer's disease (AD) with nonphysiologic overexpression of amyloid precursor protein (APP) exhibit various unnatural symptoms/dysfunctions. To overcome this issue, mice with single humanized *App* knock-in (KI) carrying Swedish (NL), Beyreuther/Iberian (F), and Arctic (G) mutations in different combinations were recently developed. The validity of these mouse models of AD from a behavioral viewpoint, however, has not been extensively evaluated. Thus, using an automated behavior monitoring system, we analyzed various behavioral domains, including executive function, and learning and memory. The *App*-KI mice carrying NL-G-F mutations showed clear deficits in spatial memory and flexible learning, enhanced compulsive behavior, and reduced attention performance. Mice carrying NL-F mutations exhibited modest abnormalities. The NL-G-F mice had a greater and more rapid accumulation of Aβ deposits and glial responses. These findings reveal that single pathologic *App*-KI is sufficient to produce deficits in broad cognitive domains and that *App*-KI mouse lines with different levels of pathophysiology are useful models of AD.

© 2016 The Author(s). Published by Elsevier Inc. This is an open access article under the CC BY-NC-ND license (http://creativecommons.org/licenses/by-nc-nd/4.0/).

1. Introduction

AD is neuropathologically characterized by the progressive deposition of extracellular 40–42 residue amyloid-β protein (Aβ; Glenner & Wong, 1984; Masters et al., 1985; Hardy & Selkoe, 2002; Kowalska, 2004) and intracellular neurofibrillary tangles comprising microtubule-associated protein tau (Grundke-Iqbal et al., 1986), followed by neuronal loss. Experimental studies of AD have largely depended on transgenic mice overexpressing APP and tau. These transgenic mice, however, exhibit artificial phenotypes, leading to misconceptions about AD pathology. The mice not only overproduce Aβ, but also other APP fragments (Hsiao et al., 1996; Sturchler-Pierrat et al., 1997), which causes multiple artificial problems, including axonal transport disruption (Taru et al., 2002). Overexpression of wild-type (WT) APP causes memory impairment without amyloid deposition, suggesting that the pathology differs from that of general AD (Chui et al., 1999), and the 40-residue isoform, Aβ40, is suggested to have a protective role in the brain (Kim et al., 2008). Inserted transgenes may affect other genes by *cis* or *trans* mechanisms (Saito et al., 2014).

To overcome these problems and identify discrete factors involved in AD pathology, three novel AD mouse models were generated by KI of a humanized Aβ sequence and familiar AD-associated mutations into the endogenous mouse *App* locus (Saito et al., 2014). The three AD models have different pathophysiologic properties in the brain. NL-F mice carrying the Swedish and Beyreuther/Iberian mutations exhibit a progressive increase in the accumulation of Aβ, a higher Aβ42:Aβ40 ratio, and amyloidosis that is restricted to cortical regions with neuroinflammatory responses. In NL-G-F mice also carrying the internal Arctic mutation within the Aβ sequence, amyloidosis is accelerated and neuroinflammation is observed in broader brain areas, including subcortical structures. NL mice carrying only the Swedish mutation, which is common in all *App* KI lines and affects β-cleavage, are used as controls to dissociate the effects of C terminal fragment-β (CTF-β) from those of Aβ (Saito et al., 2014). The neuroinflammatory response and Aβ deposition in NL mice are negligible. While Saito et al. demonstrated the advantages of the *App*-KI mice for experimental studies of AD, characterization of the behavioral phenotypes of the mice was limited.

Although dementia is a clinical hallmark of AD, broad cognitive domains, such as attention and executive functions, are also

Abbreviations: AD, Alzheimer's disease; APP, amyloid precursor protein; KI, knock-in; WT, wild-type; CTF-β, C terminal fragment-β; GFAP, glial fibrillary acidic protein; rmANOVA, repeated measures analysis of variance; MANOVA, multivariate analysis of variance; ROI, region of interest.

* Corresponding author.
E-mail addresses: masuda-akira@brain.riken.jp (A. Masuda), snow-k@brain.riken.jp (Y. Kobayashi), naomi_kogo@brain.riken.jp (N. Kogo), takasai@brain.riken.jp (T. Saito), saido@brain.riken.jp (T.C. Saido), sitohara@brain.riken.jp (S. Itohara).

http://dx.doi.org/10.1016/j.nlm.2016.07.001
1074-7427/© 2016 The Author(s). Published by Elsevier Inc.
This is an open access article under the CC BY-NC-ND license (http://creativecommons.org/licenses/by-nc-nd/4.0/).

affected in patients with AD (Lindeboom & Weinstein, 2004; Ossenkoppele et al., 2015; Perry & Hodges, 1999). Thus, to better evaluate the validity of the *App*-KI mouse models for studying AD, we extensively analyzed various cognitive domains of these mice using an automated home-cage monitoring system. Our findings support the usefulness of these mouse models for AD research.

2. Materials and methods

2.1. Animals and experimental design

The *App*-KI ($App^{NL/NL}$, $App^{NL-F/NL-F}$, *and* $App^{NL-G-F/NL-G-F}$) mice were generated as described previously (Saito et al., 2014). These mice were established as C57BL/6J congenic lines by backcrossing to C57BL/6J mice for at least 8 generations at the animal facility of the RIKEN Brain Science Institute. Mice of mixed genotypes ($App^{NL/NL}$, $App^{NL-F/NL-F}$, $App^{NL-G-F/NL-G-F}$, and WT) were co-housed, 12 animals per cage (26 cm × 37 cm × 19 cm). To reduce fighting among cage mates, especially between male mice, co-housing was initiated when the mice were young, 1–2 month-old. $App^{NL/NL}$ and WT mice were 1 month younger than $App^{NL-F/NL-F}$, *and* $App^{NL-G-F/NL-G-F}$ mice. The mice were maintained under standard housing conditions, lights on at 8:00, lights off at 20:00, and provided water and food ad libitum. All animal experiments were approved by the institutional animal care and use committee, and carried out according to the RIKEN Brain Science Institute's guidelines for animal experimentation.

2.2. Behavioral studies

The IntelliCage system (NewBehavior AG, Zurich, Switzerland, www.newbehavior.com) was described previously (Kobayashi et al., 2013; Krackow et al., 2010; Lee et al., 2015; Voikar et al., 2010). Each IntelliCage (39 cm × 58 cm × 21 cm) contains four corner chambers accessible through an open doorway, which has a ring antenna. Two doors in each corner are controlled by computers and used to control access to the water bottles. A radiofrequency identification transponder (Standard Microchip T-VA, DataMars, Switzerland & Troven, USA) was subcutaneously implanted into the mice in the dorso-cervical region under isoflurane inhalation anesthesia. Subsequently, the mice were allowed to recover for at least 1 week, in mixed genotype groups of 10–12. During all adaptation phases and tasks in the IntelliCage system, the mice were fed ad libitum with standard mouse chow and maintained on synthetic bedding (ALPHA-dri®, Shepherd Specialty Papers, Watertown, TN, USA) that was changed every 2–3 weeks depending on the task schedule. Lights were on between 08:00 and 20:00. To examine the effects of age, we conducted adaptation task three times (ages of 8–9 months, 13–14 months, and 18–19 months) and the series of experiments (Fig. 1A–E) two times (immediately after the first two adaptation tasks). For the first two phases, the task sequence was as follows: (1) place preference learning, (2) place preference reversal learning, (3) serial reaction time, (4) place avoidance learning, and (5) delay-discounting. The 3rd adaptation phase was conducted to evaluate the general behavior at the end of the whole experiment. All of the animals were tested at the same time using 8 IntelliCage Systems.

2.2.1. Adaptation phase

During first 2 days in the IntelliCage, all doors were open, providing free access to all eight drinking bottles (free adaptation). During next 4 days, all doors were closed but could be opened once per visit with a nose-poke for 5 s (nose-poke adaptation). During the last 5 days of the adaptation phase, the mice were adapted to a fixed drinking schedule (drinking session adaptation: DSA, see Fig. 1F) with doors opening in response to nose-pokes between the hours of 21:00–0:00 only.

2.2.2. Place preference learning and place preference reversal learning tasks

In this set of tasks, access to water was available in only one of four corners during the drinking sessions. The rule predicting the rewarded corner varied between tasks. In the beginning, water was available in the same corner for 7 sessions (place preference, Fig. 1A), followed by 7 sessions with water available in the opposite corner (place preference reversal, Fig. 1B). To prevent learning by imitation and to prevent overcrowding in one corner, cage mates were divided into four subgroups with different target corners.

2.2.3. Serial reaction time task to assess impulsivity and attention control

In this set of tasks, all four corners operated in the same way, 24 h per day. The first nose-poke in a visit initiated a delay period (1.0, 2.0, or 4.0 s), after which yellow LEDs were switched on and the door opened for drinking on the correct side for a certain period (0.5, 1.0, or 2.0 s). Any nose-poke during the delay period was considered a premature response, whereas the first nose-poke at the open door was counted as a correct response. Correct response latency was defined as the time that elapsed between the onset of the light stimulus and a correct response. Error responses turned the LEDs blue and then the door was closed until the mice exited the corner. The task had three phases. During the first 3 days, the delay was set to 0 s (baseline). The delays then varied randomly among 0.5, 1.0, 2.0, and 4.0 s for the rest of the task. During this period, premature responses had no consequence (pre-training). To assess impulsivity (training), during the next 7 days premature responses stopped the trial, requiring the mouse to leave the corner and to start again. To assess attention and impulsivity with high attentional load, during the next 7 days premature responses had no consequence, but a delayed nose-poke after the LED turned off stopped the trial (Fig. 1D).

2.2.4. Place avoidance learning to assess aversive spatial memory and extinction learning

This series of tasks included a training trial (Learning) followed by two probe trials (Retention and Extinction). No more than 4 animals were assigned to each corner. In the assigned corner, a nose-poke triggered an air-puff (~0.8 bar, 1-s air-puff) and the doors in this corner remained closed. The training period lasted 24 h. Thereafter, the animals were carefully removed from the IntelliCages and placed into their standard home cages. The bedding and shelter were not replaced and remained the same in the IntelliCage. The mice were subsequently reintroduced into the IntelliCage for 5 consecutive days without receiving an air puff, and with water available in all four corners. The data obtained during the first 24 h and the subsequent 5 days were analyzed to monitor the retention and extinction of place avoidance learning. Avoidance scores were quantified as the percentage of correct visits with nose-pokes.

2.2.5. Delay discounting task to assess compulsivity

In this task, all four corners operated in the same way, 24 h per day; with a given delay after onset of a visit, the doors opened spontaneously for a 5-s drinking period. To force the mice to choose either the left or right bottle, a nose-poke at any open door closed or prevented opening the door on the other side. This task was divided into two stages. In the 1st stage (training), the delay was set at 0 s, in each corner (two left corners, two right corners) one water bottle was replaced with 0.5% saccharin to allow

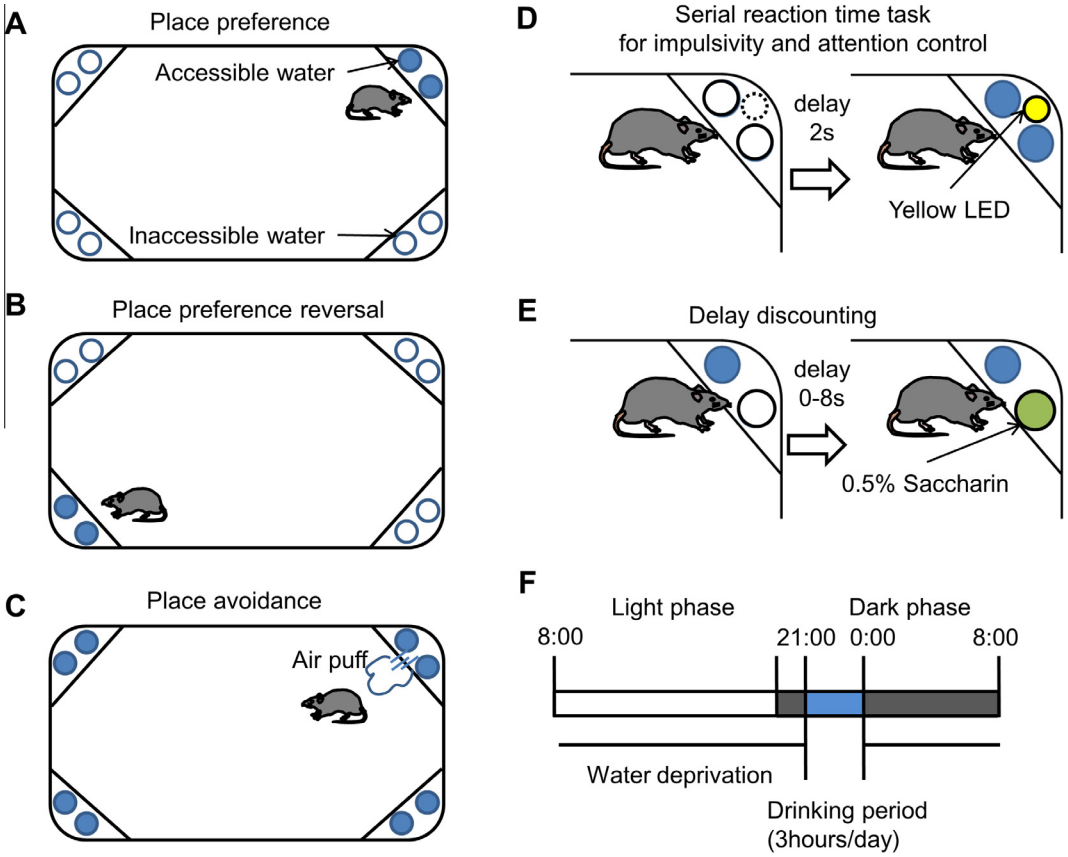

Fig. 1. Experimental design. Schematic diagrams for protocols of behavioral tasks (A–E). Place preference (PP) task in which animals have to learn the location of one accessible corner from the 4 corners (A). Place preference reversal (PPR) task in which animals have to learn the location shifted to the opposite corner (B). Place avoidance (PA) task in which animals to have to learn to avoid the location of one air-puffed corner from the 4 corners (C). Serial reaction time task to evaluate impulsivity and attention control in which animals have to wait a delay (2 s) and react quickly (within 2 s) after LED flash (0.3–1.0 s) (D). Delay discounting (DD) task to evaluate compulsivity in which animals choose immediate water access or delayed (0–8 s) 0.5% saccharin access (E). Time schedule of drinking session (F).

animals to develop a preference for saccharin over a period of at least 5 days. In the 2nd stage (delay discounting), delays to open the doors for access to the saccharin bottle were increased by 1.0 s every 24 h. Thus, after 8 days, the delay was 8 s. The saccharin preference score was calculated as: (number of licks at saccharin bottles—number of licks at water bottles)/total number of licks. Nose-pokes at the closed saccharin door during the delay period had no consequence, but were scored as a possible measure of compulsivity.

2.3. Statistical analysis of behavioral data

Data regarding the adaptation phase were analyzed using a Generalized Linear Model (GLM) and Tukey's post hoc test under FlowR (XBehavior, Zurich, Switzerland). Two-way and three-way repeated measures analysis of variance (rmANOVA), and Scheffe's post hoc tests were used to analyze the other behavioral results with Excel-based software, ExcelTokei (SSRI, Tokyo, Japan). Probability values less than 0.05 were considered statistically significant.

2.4. Histology

Another group of mice was used for the histological analyses. Immunohistochemical staining against Aβ (82E1; IBL; Japan), ionized calcium binding adaptor molecule 1 (Iba-1; Wako, Japan), and glial fibrillary acidic protein (GFAP; MAB3402; Millipore, Darmstadt, Germany) was performed in male and female mice of the 4 genotypes at 6, 12, or 18 month-old (3–5 animals each) to examine the degree of the accumulation of amyloidosis and inflammatory response by microglia and astrocytes. Paraffin-embedded mouse brain sections, two coronal sections per mouse, were immunostained using tyramide signal amplification (PerkinElmer Life Science, Waltham, USA), as previously described (Saito et al., 2014). Photographic data were captured by NanoZoomer Digital Pathology C9600 (Hamamatsu Photonics, Hamamatsu, Japan). Quantitative analysis was performed using a custom made Matlab software which defined region of interest (ROI) manually in the cortex, hippocampus and subcortical regions, made binary data under certain cut-off, and calculated percentage of occupancy area of immunoreactive signals against the ROI. Multivariate analysis of variance (MANOVA) was performed to determine the effect of genotype, age, sex, signal type, brain region and interactions among them. Scheffe's post hoc analysis also was performed accordingly.

3. Results

Each of 96 mice (12 males and 12 females per genotype) group-housed in 8 cages was implanted with a transponder for the IntelliCage system. Five mice (1NL male, 1 NL-F male, 2 NL-G-F males, and 1 NL-F female) died before the first adaptation session. Two mice (1 WT female and 1 NL-G-F female) were eliminated due to the inappropriate transponder position. By the end of the experiments, 24 mice (1 NL male, 10 NL-F males, 5 NL-G-F males, 3 WT males, 2 NL-F females, and 3 NL-G-F females) had died. The

numbers of mice analyzed are summarized in the supplemental information.

3.1. Adaptation behavior in App-KI mice

In the 1st, 2nd, and 3rd adaptation phases, free adaptation was started when the mice were 8–9 month-old, 13–14 month-old, and 18–19 month-old, respectively. All genotypes exhibited comparable activities with regard to corner visits, nose-pokes, and licks at water bottles, although significant effects of age and sex were noted, supporting the feasibility of analyzing these features in the IntelliCage from the start to the end of the experiment.

3.2. Place preference and reversal learning in App-KI mice

Spatial learning and spatial reversal learning were assessed in place preference and place preference reversal tasks, respectively. In the 1st phase, the percentage of correct visits during the place preference task was comparable among genotypes (3-way rmANOVA, day $p = 0.0001$, genotype $p = 0.07$, sex $p = 0.0003$, day × genotype $p = 0.99$, genotype × sex $p = 0.33$; Fig. 2A). If interactions between genotype and sex were rejected, the pooled data of the males and females is shown in the figures. Performance in the place preference reversal task, however, was differentially affected in NL, NL-F, and NL-G-F mice (3-way rmANOVA, day $p = 0.0001$, genotype $p = 0.45$, sex $p = 0.0001$, day × genotype $p = 0.02$, genotype × sex $p = 0.22$, simple main effect on day 1 $p = 0.0001$, day 2 $p = 0.05$, day 3–7 $p > 0.4$, post hoc, day 1, NL vs WT $p = 0.0001$, NL-F vs WT $p = 0.0001$, NL-G-F vs WT $p = 0.0001$; Fig. 2B). NL-G-F mice exhibited a slower reversal learning rate.

In the 2nd stage, performance in the place preference task was not different among genotypes (3-way rmANOVA, day $p = 0.0001$, genotype $p = 0.74$, sex $p = 0.0004$, day × genotype $p = 0.95$, genotype × sex $p = 0.23$; Fig. 2C). In the place preference reversal task, however, NL-F and NL-G-F mice exhibited marginal and severe decreases, respectively, in the percentage of correct visits over 5 days (3-way rmANOVA, day $p = 0.0001$, genotype $p = 0.005$, sex $p = 0.04$, day × genotype $p = 0.0001$, genotype × sex $p = 0.33$, simple main effect of genotype during day 1–5 $p < 0.05$, post hoc, NL vs WT $p = 0.67$, NL-F vs WT $p = 0.004$, NL-G-F vs WT $p = 0.0001$; Fig. 2D).

3.3. Impulsivity and attention control in App-KI mice

We assessed impulsivity and attention in a serial reaction time task. The animals successfully learned to wait for a delay (2 s) and react by nose-pokes to illuminated holes after 6–8 days of training. The premature poking rate gradually decreased in all groups with a modest genotype × sex interaction (3-way rmANOVA, day $p = 0.0001$, genotype $p = 0.10$, sex $p = 0.21$, day × genotype $p = 0.06$, genotype × sex $p = 0.04$). NL-F and NL-G-F males had lower premature nose-poke rates compared with WT mice (post hoc on males, NL vs WT $p = 0.77$, NL-F vs WT $p = 0.03$, NL-G-F vs WT $p = 0.01$). The interaction disappeared in the 2nd phase (3-way rmANOVA, day $p = 0.0001$, genotype $p = 0.26$, sex $p = 0.01$, day × genotype $p = 0.72$, genotype × sex $p = 0.90$).

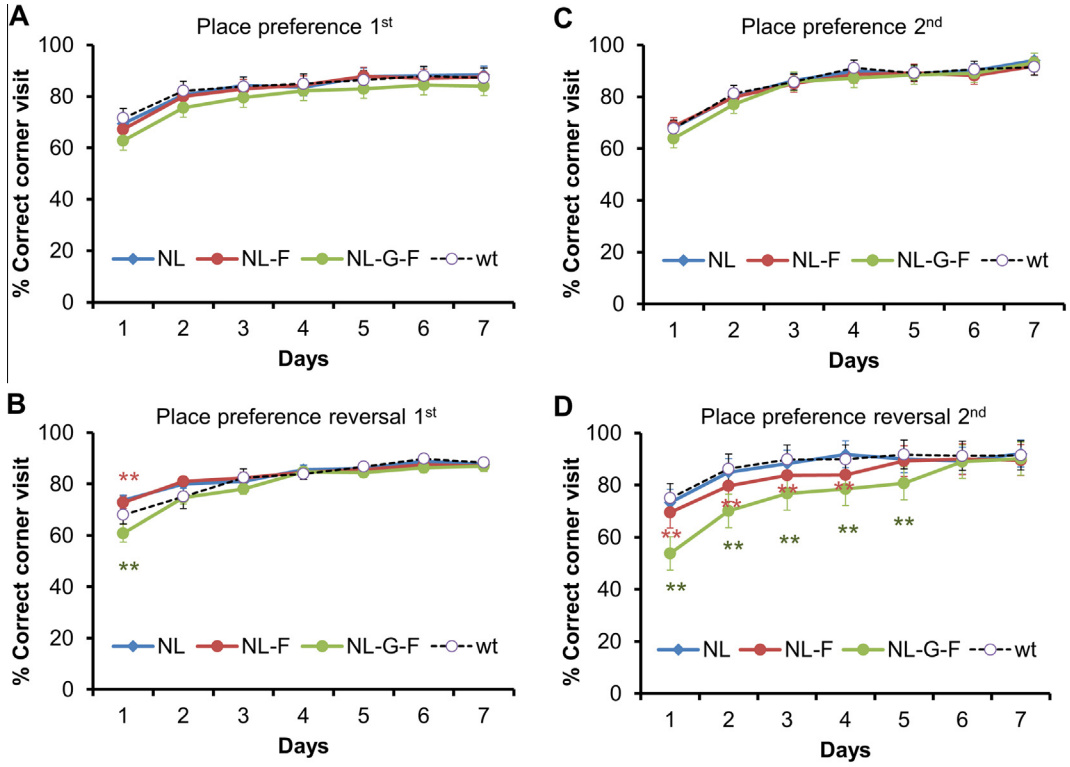

Fig. 2. Place preference learning and place reversal learning in *App*-KI mice. The percentage of correct visit in PP (A, C) and in PPR (B, D) ± SEM is presented. The statistical result for the 1st phase, PP: 3way rmANOVA, day, $F(6) = 120.46$, $p = 0.0001$, genotype, $F(3) = 2.3$, $p = 0.07$, sex, $F(1) = 3855.82$, $p = 0.0003$, day × genotype, $F(6, 3) < 0.0001$, $p = 0.99$, genotype × sex, $F(3, 1) = 1.15$, $p = 0.33$; PPR: 3way rmANOVA, day, $F(6) = 74.6$, $p = 0.0001$, genotype, $F(3) = 0.88$, $p = 0.45$, sex $F(1) = 19.07$, $p = 0.0001$, day × genotype, $F(6, 3) = 1.74$, $p = 0.02$, genotype × sex, $F(3, 1) = 1.50$, $p = 0.22$, simple main effect on day 1 $F(3) = 7.33$, $p = 0.0001$, day 2, $F(3) = 2.54$, $p = 0.05$, day 3–7, $F(3) < 0.80$, $p > 0.4$, post hoc, day 1, NL vs WT, $p = 0.0001$, NL-F vs WT, $p = 0.0001$, NL-G-F vs WT, $p = 0.0001$. The statistical result for the 2nd phase, PP: 3way rmANOVA, day $p = 0.0001$, genotype $p = 0.74$, sex $p = 0.0004$, day × genotype $p = 0.95$, genotype × sex $p = 0.23$; PPR: 3way rmANOVA, day $p = 0.0001$, genotype $p = 0.005$, sex $p = 0.04$, day × genotype $p = 0.0001$, genotype × sex $p = 0.33$, simple main effect of genotype during day 1–5 $p < 0.05$, post hoc, NL vs WT, $p = 0.67$, NL-F vs WT, $p = 0.004$, NL-G-F vs WT, $p = 0.0001$. *: $p < 0.05$; **: $p < 0.01$. Colors indicate groups of comparison: Blue: NL vs WT; Red: NL-F vs WT; Green: NL-G-F vs WT.

In the attention task conditions that required a high demand, the percentage of premature error trials was differentially modulated by genotypes in the 1st phase (3-way rmANOVA, stimulus duration (stim) $p = 0.84$, genotype $p < 0.0001$, sex $p = 0.10$, stimulus × genotype $p = 0.99$, genotype × sex $p = 0.36$), with NL having a lower percentage and NL-F and NL-G-F having higher percentages (post hoc NL vs WT $p = 0.009$, NL-F vs WT $p = 0.46$, NL-G-F vs WT $p = 0.91$, NL vs NL-F $p = 0.0008$, NL vs NL-G-F $p = 0.01$; Fig. 3A). In the 2nd phase, the percentage of premature errors was slightly decreased in NL and higher in NL-G-F, and the difference between them was statistically significant (3-way rmANOVA, stim $p = 0.40$, genotype $p = 0.006$, sex $p = 0.01$, stim × genotype $p = 0.12$, genotype × sex $p = 0.28$, post hoc NL vs WT $p = 0.40$, NL-F vs WT $p = 0.98$, NL-G-F vs WT $p = 0.13$, NL vs NL-G-F $p = 0.001$; Fig. 2C). Thus, premature responses consistently increased in NL-G-F mice, and consistently decreased in NL mice.

In the 1st phase, the accuracy, a score of attentional ability, also differed among genotypes (3-way rmANOVA, stim $p < 0.0001$, genotype $p = 0.003$, sex $p = 0.03$, stim × genotype $p = 0.81$, genotype × sex $p = 0.59$, post hoc NL vs WT $p = 0.81$, NL-F vs WT $p = 0.33$, NL-G-F vs WT $p = 0.83$, NL vs NL-G-F $p = 0.30$; Fig. 3B). Accuracy was decreased in NL-F and NL-G-F, and increased in NL. In the 2nd phase, accuracy was more severely decreased in NL-G-F, while NL and NL-F exhibited no significant differences (3-way rmANOVA, stim $p < 0.0001$, genotype $p = 0.002$, sex $p = 0.73$, stim × genotype $p = 0.006$, genotype × sex $p = 0.85$, post hoc on stim0.5 NL vs WT $p = 0.72$, NL-F vs WT $p = 0.54$, NL-G-F vs WT $p < 0.0001$; stim1 NL vs WT $p = 0.11$, NL-F vs WT $p = 0.95$, NL-G-F vs WT $p = 0.0009$, post hoc on stim0.3 NL vs WT $p = 0.86$, NL-F vs WT $p = 0.01$, NL-G-F vs WT $p = 0.41$; Fig. 3D). Therefore, a decrease in the number of accurate responses was consistently observed in NL-G-F mice in the 2nd phase.

3.4. Place avoidance learning in App-KI mice

Animals who performed a nose-poke in one of the four corners received an air-puff. In the place avoidance learning session, preference for the punished corner dropped dramatically (~3% nose-poke errors) in all genotypes (3-way rmANOVA, module $p = 0.0001$, genotype $p = 0.31$, sex $p = 0.77$, module × genotype $p = 0.05$, genotype × sex $p = 0.86$). After returning from spending 24 h in the homecage, preference for the punished corner was analyzed for aversive memory performance (retention session). In the 1st phase, avoidance behavior remained strong (~6% nose-poke errors) in WT and NL, but was significantly worse in NL-F and NL-G-F (>10% in nose-poke errors; simple main effect of genotype base $p = 0.68$, learning 0.99, retention $p = 0.001$, post hoc on retention, NL vs WT $p = 0.9$, NL-F vs WT $p = 0.0001$, NL-G-F vs WT $p = 0.001$; Fig. 4A). Extinction learning was comparable for all genotypes. In the 2nd phase, avoidance behavior was not observed in any genotype during the retention session (Fig. 4B).

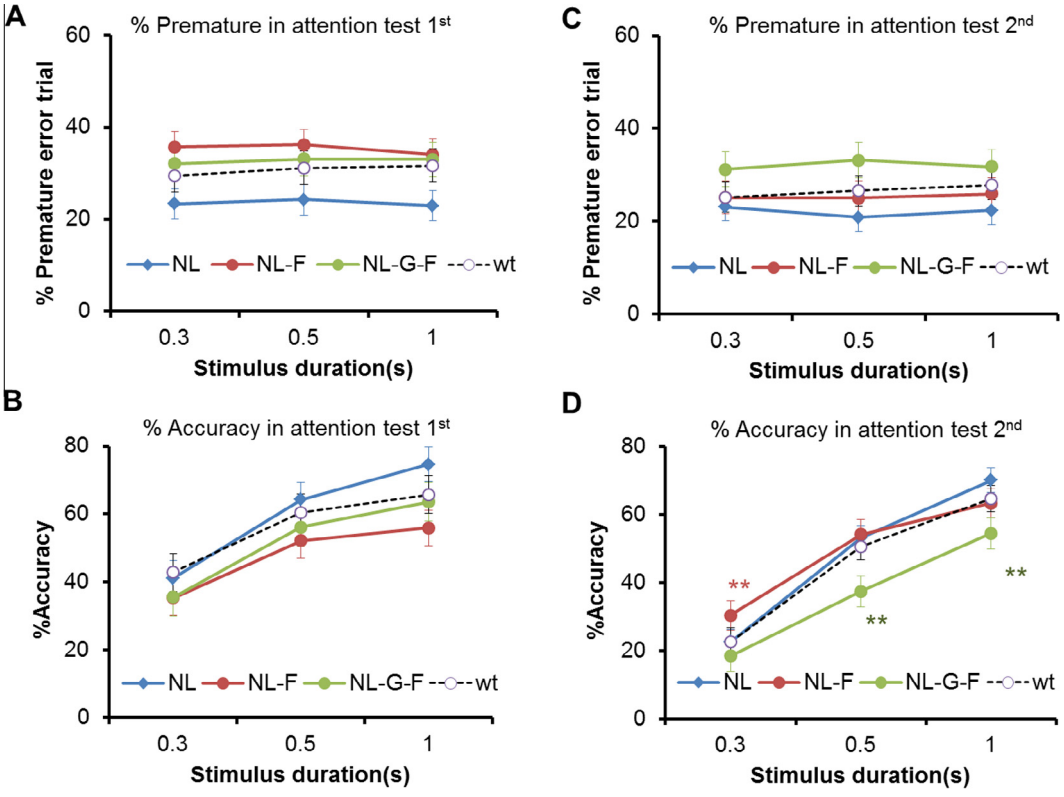

Fig. 3. Impulsivity and attention control in *App*-KI mice. The percentage of premature error trial (A, C) and that of accuracy (B, D) ± SEM is presented. The statistical result for the 1st phase, Premature %, 3way rmANOVA, stim, $F(2) = 0.17$, $p = 0.84$, genotype $F(3) = 6.77$, $p < 0.0001$, sex, $F(1) = 2.66$, $p = 0.10$, stimulus × genotype, $F(2, 3) = 0.10$, $p = 0.99$, genotype × sex, $F(3, 1) = 1.06$, $p = 0.36$, post hoc, NL vs WT, $p = 0.009$, NL-F vs WT, $p = 0.46$, NL-G-F vs WT, $p = 0.91$, NL vs NL-F, $p = 0.0008$, NL vs NL-G-F, $p = 0.01$; Accuracy, 3way rmANOVA, stim, $F(2) = 41.10$, $p < 0.0001$, genotype, $F(3) = 3.07$, $p = 0.003$, sex, $F(1) = 4.49$, $p = 0.03$, stim × genotype, $F(2, 3) = 0.48$, $p = 0.81$, genotype × sex, $F(3, 1) = 0.59$, $p = 0.59$, post hoc NL vs WT $p = 0.81$, NL-F vs WT $p = 0.33$, NL-G-F vs WT $p = 0.83$; for the 2nd phase, 3way rmANOVA, %Premature, stim, $F(2) = 0.17$, $p = 0.84$, genotype, $F(3) = 6.77$, $p = 0.004$, sex, $F(1) = 2.66$, $p = 0.01$, stim × genotype, $F(2, 3) = 0.10$, $p = 0.12$, genotype × sex, $F(3, 1) = 1.06$, $p = 0.28$, post hoc, NL vs WT, $p = 0.40$, NL-F vs WT, $p = 0.98$, NL-G-F vs WT, $p = 0.13$, NL vs NL-G-F, $p = 0.001$; %Accuracy, stim, $F(2) = 367.51$, $p < 0.0001$, genotype, $F(3) = 5.17$, $p = 0.002$, sex, $F(1) = 0.11$, $p = 0.73$, stim × genotype, $F(3, 2) = 3.18$, $p = 0.006$, genotype × sex, $F(3, 1) = 0.26$, $p = 0.85$, post hoc on stim0.3, NL vs WT, $p = 0.99$, NL-F vs WT, $p = 0.01$, NL-G-F vs WT, $p = 0.41$, post hoc on stim0.5, NL vs WT, $p = 0.72$, NL-F vs WT, $p = 0.54$, NL-G-F vs WT, $p < 0.0001$, post hoc on stim1, NL vs WT, $p = 0.11$, NL-F vs WT, $p = 0.95$, NL-G-F vs WT, $p = 0.0009$, *: $p < 0.05$; **: $p < 0.01$. Colors indicate groups of comparison: Blue: NL vs WT; Red: NL-F vs WT; Green: NL-G-F vs WT.

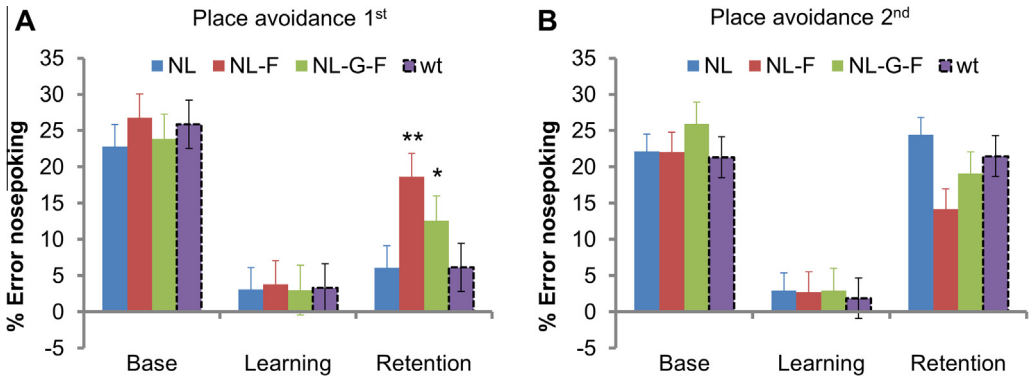

Fig. 4. Avoidance memory in *App*-KI mice. The percentage of error nosepoking in 1st phase (A) and 2nd phase (B) ± SEM is presented. The statistical result for the 1st phase, 3way rmANOVA, module, $F(3) = 62.39$, $p = 0.0001$, genotype, $F(3) = 1.21$, $p = 0.31$, sex, $F(1) = 0.08$, $p = 0.77$, module × genotype, $F(3, 3) = 1.91$, $p = 0.05$, genotype × sex, $F(3, 1) = 0.24$, $p = 0.86$, simple main effect of genotype, base, $F(3) = 0.49$ $p = 0.68$, learning, $F(3) = 0.01$, $p = 0.99$, retention, $F(3) = 5.23$, $p = 0.001$, extinction, $F(3) = 0.85$, $p = 0.46$, post hoc on retention, NL vs WT, $p = 0.9$, NL-F vs WT, $p = 0.0001$, NL-G-F vs WT, $p = 0.001$; for the 2nd phase, 3way rmANOVA, module, $F(3) = 49.94$, $p < 0.0001$, genotype, $F(3) = 2.40$, $p = 0.07$, sex, $F(1) = 1.38$, $p = 0.24$, module × genotype, $F(3, 3) = 1.07$, $p = 0.38$, genotype × sex, $F(3, 1) = 0.15$, $p = 0.92$. *: $p < 0.05$; **: $p < 0.01$.

3.5. Compulsive behavior in App-KI mice

Compulsive behavior was assessed in the delay-discounting task. In the 1st phase, the very high level of preference for saccharin (~95%) decreased as a function of the delay length with significant genotype and genotype × delay effects (3-way rmANOVA, delay $p < 0.0001$, genotype $p = 0.003$, sex $p = 0.17$, delay × genotype $p < 0.0001$, genotype × sex $p = 0.48$, simple main effect of genotype, delay 0–3 $p > 0.17$, delay 4–8 $p < 0.002$; Fig. 5A). NL-F and NL-G-F exhibited a tolerance to the decreased saccharin and maintained a high level of preference (~80% both), whereas WT and NL exhibited a significantly lower preference (~20% and 40% each; post hoc on delay 8, NL vs WT $p = 0.02$, NL-F vs WT $p < 0.0001$, NL-G-F vs WT $p < 0.0001$). In the 2nd phase, WT, NL, and NL-F exhibited a more rapidly decreasing saccharin preference than in the 1st phase. In contrast, NL-G-F maintained a strong tolerance against delay (3-way rmANOVA, delay $p < 0.0001$, genotype $p = 0.005$, sex $p = 0.0001$, delay × genotype $p < 0.0002$, genotype × sex $p = 0.66$, simple main effect of genotype, delay 0–1 $p > 0.33$, delay 3–8 $p < 0.02$, post hoc on delay 8, NL vs WT $p < 0.0001$, NL-F vs WT $p < 0.0001$, NL-G-F vs WT $p < 0.0001$; Fig. 5B).

3.6. Pathologic phenotypes among ages and sexes in humanized APP-KI mice

In tissue sections obtained from 6, 12, and 18 month-old male and female brains of the four mouse genotypes, we immunohistochemically stained Aβ with anti-Aβ (blue), microglia with anti-Iba-1 (purple), and astrocytes with anti-GFAP antibodies (green). Representative photographs of 6, 12, and 18 month-old of all genotypes are shown in Fig. 6. In NL-F mice, the accumulation of Aβ in the neocortex and hippocampus was barely detectable at 6 months of age and progressively increased by 18 months of age. In NL-G-F mice, however, a marked Aβ accumulation appeared already at 6 months of age. Aβ accumulation was difficult to detect in WT and NL mice, even at 18 months of age. An antibody to Iba-1 demonstrated a sparse distribution of microglia in WT and NL, and dense distribution in NL-F and NL-G-F mice. Especially, 12 or 18 month-old of NL-G-F, strong signals of Iba-1 were clustered in

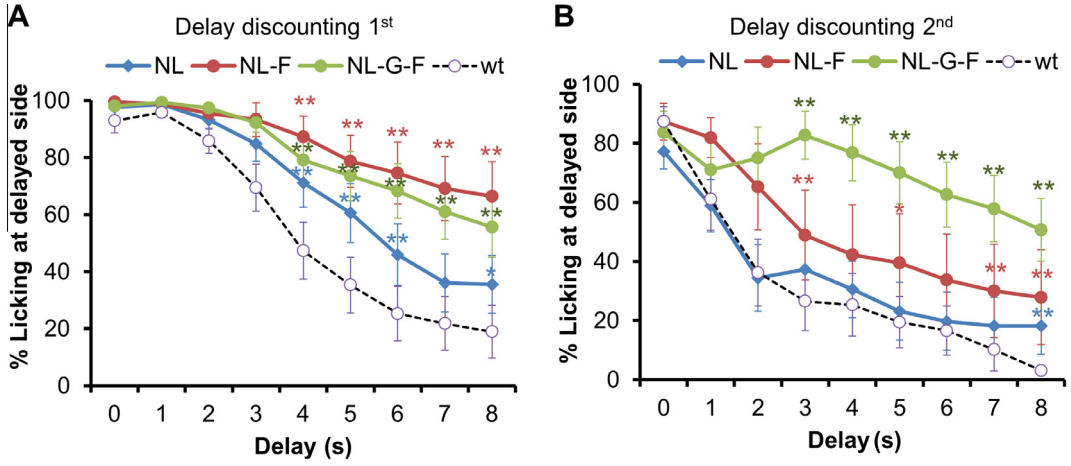

Fig. 5. Delay discounting in *App*-KI mice. The percentage of licking on 0.5% saccharin bottles in 1st phase (A) and 2nd phase (B) ± SEM is presented. The statistical result for the 1st phase, 3way rmANOVA, delay, $F(8) = 62.97$, $p < 0.0001$, genotype, $F(3) = 4.43$, $p = 0.007$, sex, $F(1) = 2.81$, $p = 0.09$, delay × genotype, $F(8, 3) = 2.50$, $p = 0.0001$, genotype × sex, $F(3, 1) = 0.95$, $p = 0.41$, simple main effect of genotype, delay 0–3, $F(3) < 1.40$, $p > 0.17$, delay 4–8, $F(3) > 4.00$, $p < 0.002$, post hoc on delay 8, NL vs WT, $p = 0.02$, NL-F vs WT, $p < 0.0001$, NL-G-F vs WT, $p < 0.0001$; for the 2nd phase, 3way rmANOVA, delay, $F(8) = 36.68$, $p < 0.0001$, genotype, $F(3) = 4.79$, $p = 0.005$, sex, $F(1) = 19.45$, $p = 0.0001$, delay × genotype, $F(8, 3) = 2.06$, $p = 0.0002$, genotype × sex, $F(3, 1) = 0.53$, $p = 0.66$, simple main effect of genotype, delay 0–1, $F(3) < 0.77$, $p > 0.33$, delay 3–8, $F(3) > 3.8$, $p < 0.02$, post hoc on delay 8, NL vs WT $p < 0.0001$, NL-F vs WT $p < 0.0001$, NL-G-F vs WT $p < 0.0001$. *: $p < 0.05$; **: $p < 0.01$. Colors indicate groups of comparison: Blue: NL vs WT; Red: NL-F vs WT; Green: NL-G-F vs WT.

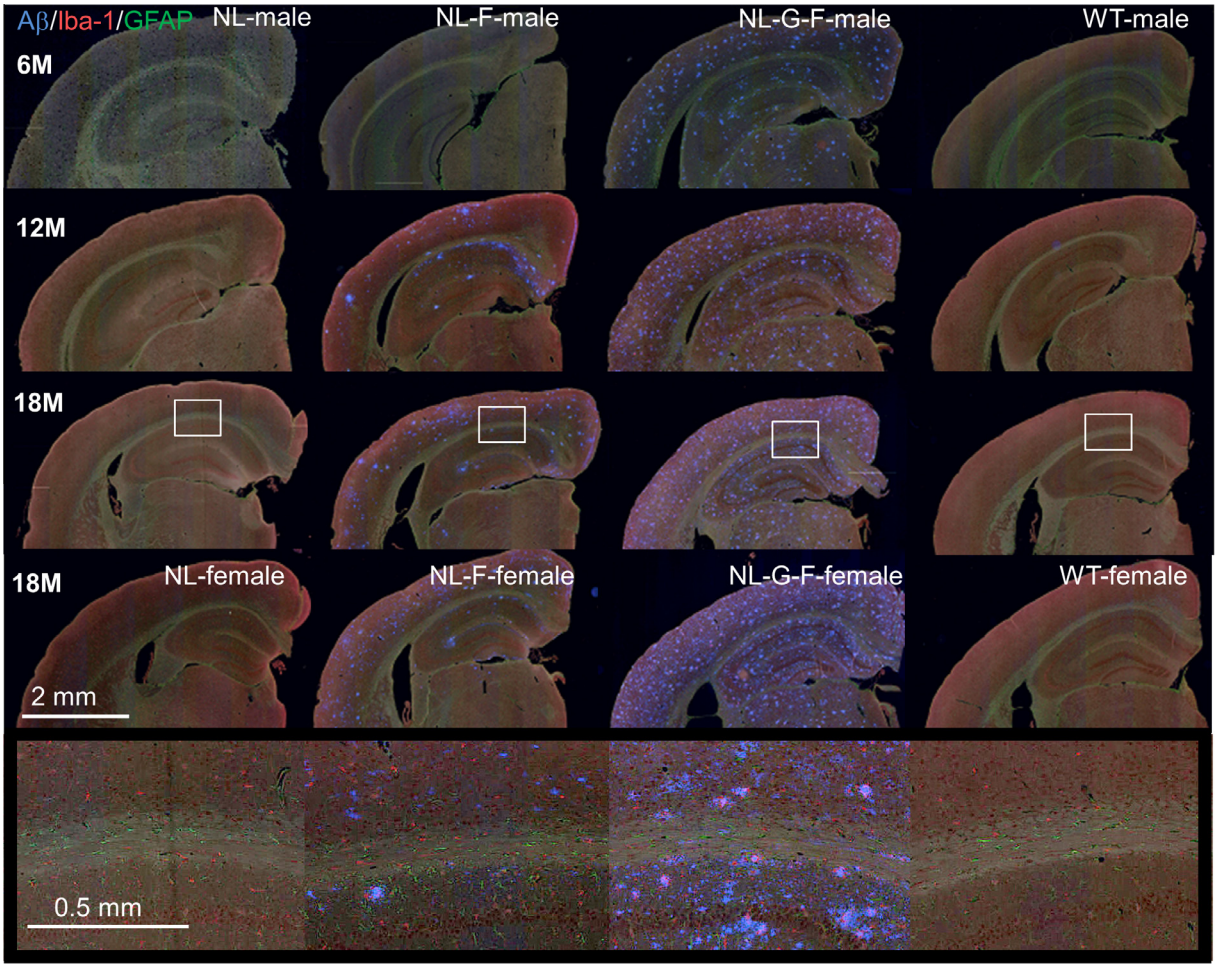

Fig. 6. Triple staining of Ab/microglia/astrocyte in *App*-KI mice. Three ages (6 M, 12 M and 18 M) of four genotypes of males and one age (18 M) of four genotypes of females are shown. The magnified images captured from enclosed areas by the white rectangles in 18 M males are shown in the lowest low. Red: Iba-1; Green: GFAP; Blue: Aβ.

the areas of Aβ deposition. The GFAP signal strength correlated positively with the signal strengths of Aβ and Iba-1, but GFAP signals were predominantly located in specific layers of the hippocampus and strong expression was found in 18 month-old of NL-G-F. Statistical analysis revealed significant effects of genotype, age, sex as well as interaction of genotype, age and sex in cortex, hippocampus and subcortical regions for percentage of occupancy area of Aβ, Iba-1 and GFAP signals (MANOVA, genotype $p < 0.0001$, age $p < 0.0001$, sex $p < 0.01$, genotype × age $p < 0.0001$, genotype × sex $p < 0.0001$, age × sex $p < 0.0001$, genotype × age × sex $p < 0.0001$, post hoc NL-G-F vs WT $p < 0.0001$, NL-G-F vs NL-F $p < 0.0001$ for Aβ, Iba-1, GFAP signals in cortex, hippocampus and subcortical regions). NL-F also showed significant increases in amyloidosis, astrocyte, and microglia compared with WT (posthoc NL-F vs WT, $p < 0.0001$ for all signals in cortex and subcortical regions; $p < 0.05$ for hippocampus, Fig. 7A–F). Apparent gender differences were observed in amyloidosis and immune responses in 18 month-old of NL-G-F mice (simple main effect of sex WT, NL and NLF $p > 0.2$, NL-G-F $p < 0.0001$, post hoc at 18 M in NL-G-F, sex $p < 0.0001$, for all signal types and brain regions, Fig. 7G–I).

4. Discussion

We performed long-term behavioral studies in both male and female *App*-KI mice, new generation mouse models of AD, using an automated behavioral assessment system at different ages (1st phase, 8–12 month-old; 2nd phase, 13–17 month-old). The IntelliCage system allowed us to record extensive and highly reproducible data under a socially rich environment in the mice with minimal human intervention (Krackow et al., 2010; Mechan, Wyss, Rieger, & Mohajeri, 2009; Voikar et al., 2010).

4.1. Behavioral symptoms of App-KI mice

Our findings indicated abnormalities of the *App*-KI mouse models in broad cognitive domains, including declined spatial reversal learning, enhanced impulsivity, declined attention control, loss of avoidance memory, and enhanced compulsivity. These behavioral aspects largely overlap with the previously reported phenotypes of transgenic AD models (Adriani et al., 2006; Romberg, Horner, Bussey, & Saksida, 2013). Symptoms of human patients with AD, including deteriorating memory loss, and enhanced impulsivity and compulsivity are well documented (Mega, Cummings, Fiorello, & Gornbein, 1996; Rochat et al., 2013).

The *App*-KI mice (both NL-F and NL-G-F) showed impaired memory in the place avoidance learning task in the 1st phase. In the 2nd phase, all genotypes, including the WT mice showed a marked deficit in the retention test, suggesting a large impact of natural aging in mice in this task. As some researchers have pointed out (Dolgin, 2013), the suitability of the task difficulty for aged animals must be considered. The performance of NL-F and NL-G-F in the place preference task was comparable with

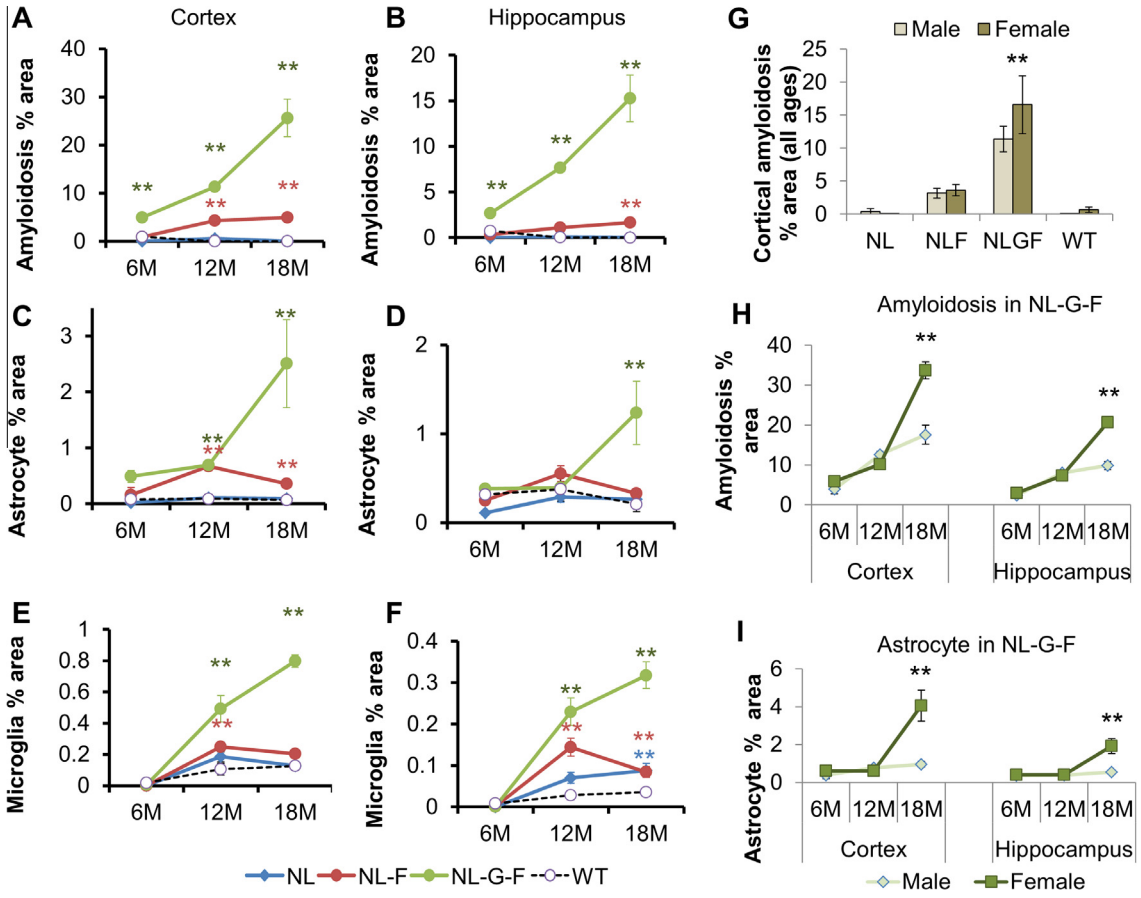

Fig. 7. Amyloidosis and immune response in *App*-KI mice. The percentage of occupancy area of Aβ, astrocyte, microglia are compared among the genotypes, age, sex. (MANOVA, genotype $F(3) > 19.9$, $p < 0.0001$, age $F(2, 53) > 10.1$, $p < 0.0001$, sex $F(1, 53) > 7.7$, $p < 0.01$, genotype × age $F(6, 53) > 12.8$, $p < 0.0001$, genotype × sex $F(3, 53) > 7.5$, $p < 0.0001$, genotype × age × sex $F(6, 53) > 4.1$, $p < 0.0001$, post hoc NL-G-F vs WT, $p < 0.0001$, NL-G-F vs NL-F, $p < 0.0001$ for Ab, Iba-1, GFAP signals in cortex, hippocampus and subcortical regions). NL-F also showed significant increases in amyloidosis, astrocyte, and microglia compared with WT (posthoc NL-F vs WT, $p < 0.0001$ for all signals in cortex and subcortical regions; $p < 0.05$ for hippocampus, Fig. 7A–F). Apparent gender differences were observed in amyloidosis and immune responses in 18 month-old of NL-G-F mice (simple main effect of sex in WT, NL and NL-F $F(1, 53) < 0.62$, $p > 0.43$, in NL-G-F $F(1, 53) = 42.7$, $p < 0.0001$, post hoc at 18 M in NL-G-F, sex $F(1, 13) = 60.9$, $p < 0.0001$, for cortical amyloidosis, Fig. 7G–I). *: $p < 0.05$; **: $p < 0.01$. Colors indicate groups of comparison: Blue: NL vs WT; Red: NL-F vs WT; Green: NL-G-F vs WT.

WT and NL mice in both the 1st and 2nd phases, although NL-G-F mice exhibited a modest, but not significant, decrease in the number of correct responses in both the 1st and 2nd phases. *App*-KI mice exhibited impaired flexibility in the place preference reversal task. In the 1st phase, NL-G-F mice had impaired performance in place preference reversal. In the 2nd phase, NL-G-F mice had severe deficits, and NL-F mice had modest deficits. A previous study using the IntelliCage system showed impaired place preference reversal learning in 10-month-old female transgenic (Tg)-ArcSwe mice (Codita et al., 2010). Together, these results suggest that the Beyreuther/Iberian mutations impair behavioral flexibility and that the Arctic mutation accelerates impairments in behavioral flexibility in an age-dependent manner.

App-KI mice exhibited increased impulsivity and attention deficits. A previous study using a touchscreen-based 5-choice serial reaction time task showed that 3xTg mice make fewer accurate responses compared with controls (Romberg, Mattson, Mughal, Bussey, & Saksida, 2011). Similarly, in the present study, NL-G-F mice, but not NL-F mice had low accurate responses, suggesting that the effects of the Arctic mutation on attentional control are similar to those of the combinational factors of 3xTg.

The NL-F and NL-G-F mice exhibited enhanced compulsivity in the delay-discounting task. A higher number of perseverative responses, persistent responses without reward, were also observed in 3xTg mice in the 5-choice serial reaction time task (Romberg et al., 2011) and transgenic APP-Arc mice in a previous IntelliCage study (Codita et al., 2010). These findings suggest that the Beyreuther/Iberian mutations impair control of compulsivity. Compulsivity can be affected by modulation of reversal learning (Endo et al., 2012; Izquierdo & Jentsch, 2012). NL-F mice showed normal or relatively better performance in the 1st phase of the place preference reversal task, indicating that enhanced compulsivity is not due to a reversal learning inability. Compulsive behavior is frequently observed in dementia syndromes (Mendez, Cherrier, & Perryman, 1997), but is relatively rare in human AD.

4.2. Relation between pathology and behaviors

The NL-G-F mice begin accumulating detectable levels of Aβ at an earlier age (6 month-old) than the NL-F (12–18 month-old), and the degree of the accumulation was also much larger. In contrast, behavioral abnormalities in NL-F were detectable by 10 months of age, which is relatively younger than the age suggested in a previous study (Saito et al., 2014). Interestingly, the Aβ deposition level in NL-F at any age was much milder than that in NL-G-F, but enhanced compulsivity was profound in NL-F at 12 months of age. One hypothesis is that even relatively moderate Aβ accumulation is sufficient to induce behavioral abnormalities, and some other unknown factor(s) in the early stage of Aβ accumulation may also independently affect the regulation of compulsivity. For

example, a prospective longitudinal study analyzing large cohorts with autosomal dominant AD suggests that various biological changes such as increased Aβ42 in cerebral spinal fluid, brain atrophy, and decreased glucose metabolism are detectable 25–15 years before the expected onset of AD symptoms, which is based on the age of symptom onset in a parent (Bateman et al., 2012). Impaired episodic memory and cognitive impairment can be detected 10 years and 5 years before the onset, respectively (Bateman et al., 2012). Biological cascade at presimptomatic period may be important for the early disturbance in memory and cognitive functions.

Reversal learning and attention deficits were affected later than compulsivity in the NL-F and NL-G-F mice, which likely reflects differences in the brain regions responsible for these behaviors. The sensitivity and vulnerability against Aβ also probably differ by brain region. For example, a specific peptidase, neprilysin, degrades amyloid deposits (Iwata et al., 2001) and neprilysin is strongly expressed in subcortical regions. Reversal learning and attention control are rooted in various overlapping brain regions, including the cortico-striato circuit (Clarke et al., 2005; Figee, Wielaard, Mazeheri, & Denys, 2013; Squire, Noudoost, Schafer, & Moore, 2013) and some other mutually exclusive regions. Differences in sensitivity to Aβ in each brain region may lead to different time-course of abnormalities in each behavioral aspect.

4.3. Minor sex-dependent effect on cognitive behavior in App-KI mice

Previous studies using transgenic models indicate that female AD model mice are more vulnerable to AD than males (King et al., 1999). The present study did not replicate these sex differences in behavioral aspects even though we confirmed the exacerbated pathological features in aged females of NL-G-F mice. We performed a 3-way ANOVA to detect a sex effect as well as a genotype × sex interaction, whereas a previous study compared the genotype effect in males and females separately, but did not directly assess the genotype × sex interaction. In addition, we used humanized *App*-KI mice, which exhibit mutations only in the APP sequence and do not exhibit presenilin or tau mutations. Taken together, our results suggest that the effect of pathologic Aβ accumulations on behavior has low sensitivity to sex-dependent factors, which may be due to the lack of presenilin and/or tau mutations.

Sex-specific inflammatory responses have been reported. In triple-transgenic 3xTg AD mice, Tg males show more evident age-dependent impairments in neuroimmunoendocrine responses than females (Giménez-Llort, Arranz, Maté, & De la Fuente, 2008). This is consistent with a report that the level of amyloid deposition is greater in female APP Tg mice compared with same-age male APP Tg mice (Wang, Tanila, Puollväli, Kadish, & Groen, 2003). Our histopathologic study also found the increased amyloidosis and inflammatory responses in 18 month-old female NL-G-F mice than male mice. This indicates that single knock-in of pathological *App* is sufficient to induce sex-dependent pathology.

Together, our findings support the feasibility of using *App*-KI mice as AD models. These three *App*-KI mice with different phenotypes in Aβ deposition, neuroinflammation, and behavioral deficits are useful for analyzing the environmental and genetic factors involved in the pathogenesis of AD and potential therapeutic strategies.

Acknowledgements

We thank Dr. Hans-Peter Lip, University of Zürich, and Dr. Sven Krackow, XBehavior, for helpful comments and statistical advices. We also acknowledge Naomi Mihira and Yukio Matsuba for technical supports. This work was supported in part by "Funding Program for World-Leading Innovative R&D on Science and Technology (FIRST Program)." The authors declare no competing financial interests.

References

Adriani, W., Ognibene, E., Heuland, E., Ghirardi, O., Caprioli, A., & Laviola, G. (2006). Motor impulsivity in APP-SWE mice: A model of Alzheimer's disease. *Behavioural Pharmacology, 17*(5–6), 525–533.

Bateman, R. J., Xiong, C., Benzinger, T. L. S., Fagan, A. M., Goate, A., Fox, N. C., ... Morris, J. C. (2012). Clinical and biomarker changes in dominantly inherited Alzheimer's disease. *The New England Journal of Medicine, 367*(9), 795–804.

Chui, D. H., Tanahashi, H., Ozawa, K., Ikeda, S., Checler, F., Ueda, O., ... Tabira, T. (1999). Transgenic mice with Alzheimer presenilin 1 mutations show accelerated neurodegeneration without amyloid plaque formation. *Nature Medicine, 5*(5), 560–564.

Clarke, H. F., Walker, S. C., Crofts, H. S., Dalley, J. W., Robbins, T. W., & Roberts, A. C. (2005). Prefrontal serotonin depletion affects reversal learning but not attentional set shifting. *The Journal of Neuroscience: The Official Journal of the Society for Neuroscience, 25*(2), 532–538.

Codita, A., Gumucio, A., Lannfelt, L., Gellerfors, P., Winblad, B., Mohammed, A. H., & Nilsson, L. N. G. (2010). Impaired behavior of female tg-ArcSwe APP mice in the IntelliCage: A longitudinal study. *Behavioural Brain Research, 215*(1), 83–94.

Dolgin, E. (2013). Old mice require new experimental tricks to study aging process. *Nature Medicine, 19*(5), 518–519.

Endo, T., Kakeyama, M., Uemura, Y., Haijima, A., Okuno, H., & Bito, H. (2012). Executive function deficits and social-behavioral abnormality in mice exposed to a low dose of dioxin In utero and via lactation. *PLoS ONE, 7*(12), e50741.

Figee, M., Wielaard, I., Mazaheri, A., & Denys, D. (2013). Neurosurgical targets for compulsivity: What can we learn from acquired brain lesions? *Neuroscience and Biobehavioral Reviews, 37*(3), 328–339.

Giménez-Llort, L., Arranz, L., Maté, I., & De la Fuente, M. (2008). Gender-specific neuroimmunoendocrine aging in a triple-transgenic 3xTg-AD mouse model for Alzheimer's disease and its relation with longevity. *NeuroImmunoModulation, 15*(4–6), 331–343.

Glenner, G. G., & Wong, C. W. (1984). Alzheimer's disease and Down's syndrome: Sharing of a unique cerebrovascular amyloid fibril protein. *Biochemical and Biophysical Research Communications, 122*(3), 1131–1135.

Grundke-Iqbal, I., Iqbal, K., Tung, Y. C., Quinlan, M., Wisniewski, H. M., & Binder, L. I. (1986). Abnormal phosphorylation of the microtubule-associated protein tau (tau) in Alzheimer cytoskeletal pathology. *Proceedings of the National Academy of Sciences, 83*(13), 4913–4917.

Hardy, J., & Selkoe, D. J. (2002). The amyloid hypothesis of Alzheimer's disease: Progress and problems on the road to therapeutics. *Science (New York, N.Y.), 297*(5580), 353–356.

Hsiao, K., Chapman, P., Nilsen, S., Eckman, C., Harigaya, Y., Younkin, S., ... Cole, G. (1996). Correlative memory deficits, Abeta elevation, and amyloid plaques in transgenic mice. *Science (New York, N.Y.), 274*(5284), 99–102.

Iwata, N., Tsubuki, S., Takaki, Y., Shirotani, K., Lu, B., Gerard, N. P., ... Saido, T. C. (2001). Metabolic regulation of brain Abeta by neprilysin. *Science (New York, N.Y.), 292*(5521), 1550–1552.

Izquierdo, A., & Jentsch, J. D. (2012). Reversal learning as a measure of impulsive and compulsive behavior in addictions. *Psychopharmacology (Berl), 219*(2), 607–620.

Kim, J., Miller, V. M., Levites, Y., West, K. J., Zwizinski, C. W., Moore, B. D., ... Golde, T. E. (2008). BRI2 (ITM2b) inhibits Abeta deposition in vivo. *The Journal of Neuroscience, 28*(23), 6030–6036.

King, D. L., Arendash, G. W., Crawford, F., Sterk, T., Menendez, J., & Mullan, M. J. (1999). Progressive and gender-dependent cognitive impairment in the APPSW transgenic mouse model for Alzheimer's disease. *Behavioural Brain Research, 103*(2), 145–162.

Kobayashi, Y., Sano, Y., Vannoni, E., Goto, H., Suzuki, H., Oba, A., ... Itohara, S. (2013). Genetic dissection of medial habenula-interpeduncular nucleus pathway function in mice. *Frontiers in Behavioral Neuroscience, 7*, 17.

Kowalska, A. (2004). Genetic basis of neurodegeneration in familial Alzheimer's disease. *Polish Journal of Pharmacology, 56*, 171–178.

Krackow, S., Vannoni, E., Codita, A., Mohammed, A. H., Cirulli, F., Branchi, I., ... Lipp, H.-P. (2010). Consistent behavioral phenotype differences between inbred mouse strains in the IntelliCage. *Genes, Brain, and Behavior, 9*(7), 722–731.

Lee, K., Kobayashi, Y., Seo, H., Kwak, J.-H., Masuda, A., Lim, C.-S., ... Itohara, S. (2015). Involvement of cAMP-guanine nucleotide exchange factor II in hippocampal long-term depression and behavioral flexibility. *Molecular Brain, 8*(1), 38.

Lindeboom, J., & Weinstein, H. (2004). Neuropsychology of cognitive ageing, minimal cognitive impairment, Alzheimer's disease, and vascular cognitive impairment. *European Journal of Pharmacology, 490*(1–3), 83–86.

Masters, C. L., Simms, G., Weinman, N. A., Multhaup, G., McDonald, B. L., & Beyreuther, K. (1985). Amyloid plaque core protein in Alzheimer disease and Down syndrome. *Proceedings of the National Academy of Sciences, 82*(12), 4245–4249.

Mechan, A. O., Wyss, A., Rieger, H., & Mohajeri, M. H. (2009). A comparison of learning and memory characteristics of young and middle-aged wild-type mice in the IntelliCage. *Journal of Neuroscience Methods, 180*(1), 43–51.

Mega, M. S., Cummings, J. L., Fiorello, T., & Gornbein, J. (1996). The spectrum of behavioral changes in Alzheimer's disease. *Neurology, 46*(1), 130–135.

Mendez, M. F., Cherrier, M. M., & Perryman, K. M. (1997). Differences between Alzheimer's disease and vascular dementia on information processing measures. *Brain and Cognition, 34*(2), 301–310.

Ossenkoppele, R., Pijnenburg, Y. A. L., Perry, D. C., Cohn-Sheehy, B. I., Scheltens, N. M. E., Vogel, J. W., ... Rabinovici, G. D. (2015). The behavioural/dysexecutive variant of Alzheimer's disease: Clinical, neuroimaging and pathological features. *Brain: A Journal of Neurology, 138*(Pt 9), 2732–2749.

Perry, R. J., & Hodges, J. R. (1999). Attention and executive deficits in Alzheimer's disease: A critical review. *Brain, 122*(3), 383–404.

Rochat, L., Billieux, J., Juillerat Van der Linden, A.-C., Annoni, J.-M., Zekry, D., Gold, G., & Van der Linden, M. (2013). A multidimensional approach to impulsivity changes in mild Alzheimer's disease and control participants: Cognitive correlates. *Cortex; A Journal Devoted to the Study of the Nervous System and Behavior, 49*(1), 90–100.

Romberg, C., Horner, A. E., Bussey, T. J., & Saksida, L. M. (2013). A touch screen-automated cognitive test battery reveals impaired attention, memory abnormalities, and increased response inhibition in the TgCRND8 mouse model of Alzheimer's disease. *Neurobiology of Aging, 34*(3), 731–744.

Romberg, C., Mattson, M. P., Mughal, M. R., Bussey, T. J., & Saksida, L. M. (2011). Impaired attention in the 3xTgAD mouse model of Alzheimer's disease: Rescue by donepezil (Aricept). *The Journal of Neuroscience: The Official Journal of the Society for Neuroscience, 31*(9), 3500–3507.

Saito, T., Matsuba, Y., Mihira, N., Takano, J., Nilsson, P., Itohara, S., ... Saido, T. C. (2014). Single App knock-in mouse models of Alzheimer's disease. *Nature Neuroscience, 17*(5), 661–663.

Squire, R. F., Noudoost, B., Schafer, R. J., & Moore, T. (2013). Prefrontal contributions to visual selective attention. *Annual Review of Neuroscience, 36*, 451–466.

Sturchler-Pierrat, C., Abramowski, D., Duke, M., Wiederhold, K. H., Mistl, C., Rothacher, S., ... Sommer, B. (1997). Two amyloid precursor protein transgenic mouse models with Alzheimer disease-like pathology. *Proceedings of the National Academy of Sciences of the United States of America, 94*(24), 13287–13292.

Taru, H., Iijima, K.-I., Hase, M., Kirino, Y., Yagi, Y., & Suzuki, T. (2002). Interaction of Alzheimer's beta -amyloid precursor family proteins with scaffold proteins of the JNK signaling cascade. *The Journal of Biological Chemistry, 277*(22), 20070–20078.

Voikar, V., Colacicco, G., Gruber, O., Vannoni, E., Lipp, H.-P., & Wolfer, D. P. (2010). Conditioned response suppression in the IntelliCage: Assessment of mouse strain differences and effects of hippocampal and striatal lesions on acquisition and retention of memory. *Behavioural Brain Research, 213*(2), 304–312.

Wang, J., Tanila, H., Puoliväli, J., Kadish, I., & van Groen, T. (2003). Gender differences in the amount and deposition of amyloidβ in APPswe and PS1 double transgenic mice. *Neurobiology of Disease, 14*(3), 318–327.